Nanoscale Res Lett (2010) 5:1387–1392
DOI 10.1007/s11671-010-9615-0

NANO EXPRESS

Synthesis of $ZnGa_2O_4$ Hierarchical Nanostructure by Au Catalysts Induced Thermal Evaporation

Xiao Meng Chen · Guang Tao Fei · Jian Yan · Yan Qing Zhu · Li De Zhang

Received: 14 March 2010 / Accepted: 16 April 2010 / Published online: 6 July 2010

Abstract In this paper, $ZnGa_2O_4$ hierarchical nanostructures with comb-like morphology are fabricated by a simple two-step chemical vapor deposition (CVD) method: first, the Ga_2O_3 nanowires were synthesized and employed as templates for the growth of $ZnGa_2O_4$ nanocombs; then, the as-prepared Ga_2O_3 nanowires were reacted with ZnO vapor to form $ZnGa_2O_4$ nanocombs. Before the reaction, the Au nanoparticles were deposited on the surfaces of Ga_2O_3 nanowires and used as catalysts to control the teeth growth of $ZnGa_2O_4$ nanocombs. The as-prepared $ZnGa_2O_4$ nanocombs were highly crystallized with cubic spinel structure. From the photoluminescence (PL) spectrum, a broad band emission in the visible light region was observed of as-prepared $ZnGa_2O_4$ nanocombs, which make it promising application as an optical material.

Keywords $ZnGa_2O_4$ · Hierarchical nanostructure · Chemical vapor deposition · Au catalyst

Introduction

With the development of nanotechnology, low dimensional nanostructures are desired nanobuilding blocks for the assembly of various electronic and optical nanodevices to realize their potential applications [1–4]. So far, many kinds of low dimensional nanostructures, such as 1-D nanowires, nanorods, nanobelts, or 2-D nanosheets have been synthesized and studied. For low dimensional nanostructures, the morphology, structure, and size may sensitively affect the properties of nanostructures, so it is of high importance to fabricate nanostructures with designed morphology and size in a controlled way.

$ZnGa_2O_4$ is an important semiconducting material for applications in flat-panel displays as a blue phosphor, for its good cathode luminescence characteristics at low driving voltage and with more stability in high vacuum than sulfide-based phosphors [5–12]. Moreover, since $ZnGa_2O_4$ has a low resistivity at room temperature [6], it is also a promising transparent conducting oxide (TCO) when transparency through the violet to near UV region is desired. $ZnGa_2O_4$ are recently proven to be a promising photocatalyst for environmental purification of air and water polluted by organic compounds due to its photo-electrochemical properties [13, 14], it may have potential use in the environmental purification field.

In the past few years, $ZnGa_2O_4$ nanowires and thin films have been synthesized using various methods such as solid-state reaction [7, 15, 16], sputtering [8], sol–gel processing [17], electrophoresis [18], pulsed laser deposition [19], thermal evaporation [20, 21], and chemical vapor deposition [22–26]. However, the synthesis of hierarchical $ZnGa_2O_4$ nanostructures has not been investigated yet. As is known, the hierarchical nanostructures will improve the performance of materials in the field of optics, electronics, and catalysis [27–29]. In this paper, we present a novel route for the synthesis of $ZnGa_2O_4$ nanocombs in a controlled way by a simple CVD method. The optical properties of $ZnGa_2O_4$ nanocombs have been studied by the room-temperature PL, a broad band emission with the full wavelength at half maximum of about 175 nm in visible light region can be observed.

X. M. Chen · G. T. Fei (✉) · J. Yan · Y. Q. Zhu · L. De Zhang
Key Laboratory of Materials Physics and Anhui Key Laboratory of Nanomaterials and Nanotechnology, Institute of Solid State Physics, Hefei Institutes of Physical Science, Chinese Academy of Sciences, 230031 Hefei, People's Republic of China
e-mail: gtfei@issp.ac.cn

Experimental Section

The synthesis of the $ZnGa_2O_4$ nanocombs was carried out in a conventional horizontal furnace in two steps, and the Ga_2O_3 nanowires were first synthesized as the templates for the following growth of $ZnGa_2O_4$ nanocombs. In brief, an alumina tube (outer diameter: 25 mm; length: 80 cm) was mounted horizontally inside a single-zone high temperature resistance furnace. For the synthesis of Ga_2O_3 nanowires, a mixture of Ga_2O_3 and active carbon powders (molar ratio 1:2) was put in an alumina boat that was located at the center of the furnace tube, and a silicon wafer coated with ~3-nm Au film was placed downstream at a distance of 4 cm. Before heating, the system was purged with 100-sccm (standard cubic centimeter per minute) high-purity argon (Ar, 99.999%) for 1 h. The furnace was heated up to 1,000°C and kept at this temperature for 30 min. After the furnace cooled down to room temperature, a layer of white products was deposited on the Si wafer.

The as-prepared Ga_2O_3 nanowires on Si substrate were coated with ~2-nm Au film through an ion coater Eiko-IB-3 (Vacuum: 0.2 Torr, electricity current: 6 mA for 10 s), and then annealed at 1,000°C for 30 min under the high-purity Ar gas surrounding. After annealing, Au particles formed from the congregation of Au film were well arranged on the side surface of the Ga_2O_3 nanowires, and they act as the secondary catalysts guiding the teeth growth.

Then, one gram of ZnO and active carbon powders (molar ratio 1:2) was put in an alumina boat placed at the center of an alumina tube. The Ga_2O_3 nanowires with the Au nanoparticles on its side were placed downstream at a distance of 4 cm. Before heating, a carrying gas (100 sccm Ar) was introduced into the tube for about 30 min. Under the constant flow of Ar, the furnace was rapidly raised to 850°C in 10 min and kept at this temperature for 10 min. After reaction, white products on the Si substrate were obtained.

The as-prepared samples were characterized using an X-ray diffraction (XRD, Philips X'pert PRO) with Cu K_α radiation, field-emission scanning electron microscopy (FE-SEM, Sirion 200), high-resolution transmission electron microscopy (HRTEM, JEOL-2010), and photoluminescence (PL) spectrometer (JY Fluogolog-3-TAU, Xe lamp) at room temperature.

Results and Discussion

Figure 1 is the characterization of the Ga_2O_3 nanowires synthesized in the first step. From Fig. 1a, it can be seen that the diameter of nanowires is about 80–100 nm and the length of nanowires is up to several tens of micrometers. Au particle can be found on the top of each nanowire, and the diameter of the nanowire is consistent with the size of Au particle, which indicates that the growth of Ga_2O_3 nanowires follows the VLS mechanism [30]. The XRD pattern in Fig. 1b indicates that all the diffraction peaks except the peak from the Si (111) substrate can be indexed as monoclinic structure β-Ga_2O_3 (JCPDS: 11-0370) with lattice constants of $a = 5.80$ Å, $b = 3.04$ Å, $c = 12.23$ Å, and $\beta = 103.7°$.

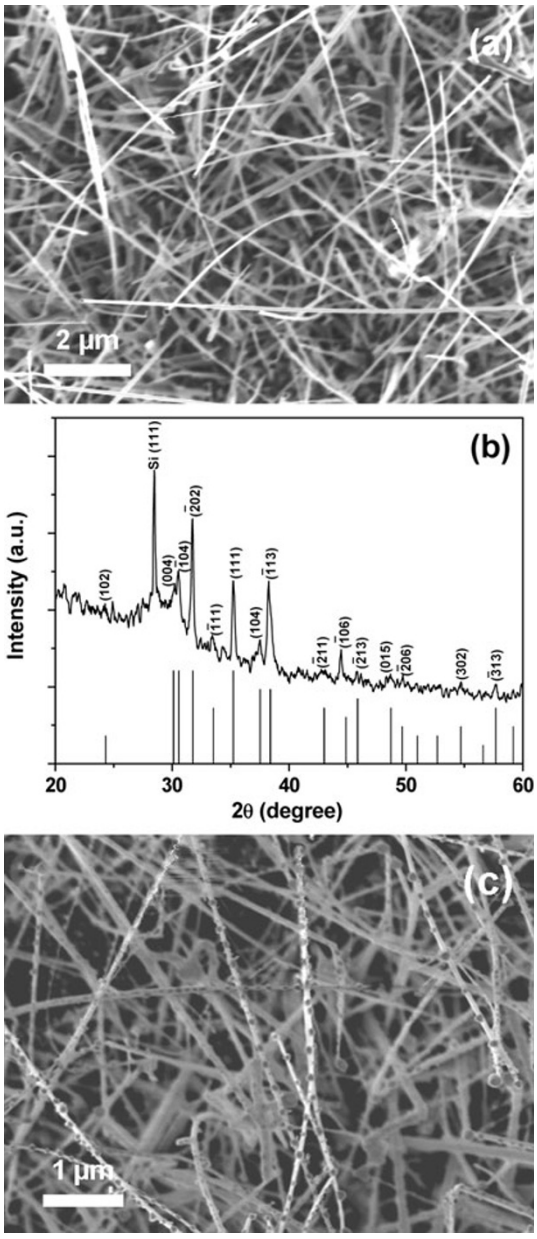

Fig. 1 **a** FE-SEM image of the Ga_2O_3 nanowires; **b** XRD pattern of as-prepared Ga_2O_3 nanowires; **c** FE-SEM image of Au nanoparticles on Ga_2O_3 nanowires after annealing at 1,000°C for 30 min

In recent reports, Ga_2O_3 nanowires are employed to synthesis $ZnGa_2O_4$ nanowires through high temperature reaction with ZnO vapor [16, 21]. Inspired by this, here in this paper, Ga_2O_3 nanowires were used as templates for the growth of $ZnGa_2O_4$ nanocombs. Catalyst induced growth is well known as a powerful method to control the growth of 1-D nanostructures. In order to guide the growth of the teeth of nanocombs, Au nanoparticles are introduced in our experiment. A thin layer of Au was deposited on the surface of as-grown Ga_2O_3 nanowires. After annealed at 1,000°C for 30 min, Au layer congregate into nanoparticles. As shown in Fig. 1c, Au nanoparticles arrange regularly on the side surface of Ga_2O_3 nanowires, which may derive from the difference of surface energy of Ga_2O_3 crystal planes. Orderly arrange of Au nanoparticles on the specific plane of Ga_2O_3 nanowire may have low energy and remain stable. This phenomenon is used to obtain the controlled growth of the teeth of $ZnGa_2O_4$ nanocombs. In addition, the annealing process is very important to get comb-like Ga_2O_3 nanostructures. We will discuss in the following.

Figure 2 shows the morphologies and crystalline structure characterization of the as-synthesized $ZnGa_2O_4$ products using FE-SEM and XRD. Figures 2a and b show the low- and high-magnification FE-SEM images of as-prepared products, which reveal that a large amount hierarchical nanostructures with comb-like morphologies are formed. The nanoteeth on the backbones in our fabricated samples are not as densely aligned as that in other nanocomb materials. The nanocombs are several tens of micrometers long with the teeth about 200 nm in length, and the teeth are orderly arranged on one side of nanocomb. The FE-SEM image shows clearly that there is a nanoparticle on the tip of each tooth. The particle was confirmed to be Au by EDS spectra in the following TEM analysis. Figure 2c shows the corresponding XRD pattern, most of the main diffraction peaks can be indexed to cubic spinel structure $ZnGa_2O_4$ (JCPDS: 38-1240) with lattice constant of $a = 8.334$ Å, except the peaks from Si(111) substrate and Au nanoparticles (111) diffraction.

Figure 3a shows a typical TEM image of a single-$ZnGa_2O_4$ nanocomb, indicating that the diameter of the tooth gradually increasing from the tip to the bottom. Figure 3b–e are the EDS spectra acquired from the marked regions 1 to 4 in Fig. 3a. The copper and carbon signals in EDS spectra are caused by the copper grids used in TEM observation. The EDS spectrum of region 1 confirms that the particle on the tip of the tooth is Au catalyst. Apparently, the growth of the teeth is induced by the Au catalyst. From the EDS spectra of region 2 to 4, it can be found that the atomic ratio of Zn:Ga in all these regions are close to 1:2. These results further confirm that the nanocomb is zcomposed of $ZnGa_2O_4$. The high-resolution TEM

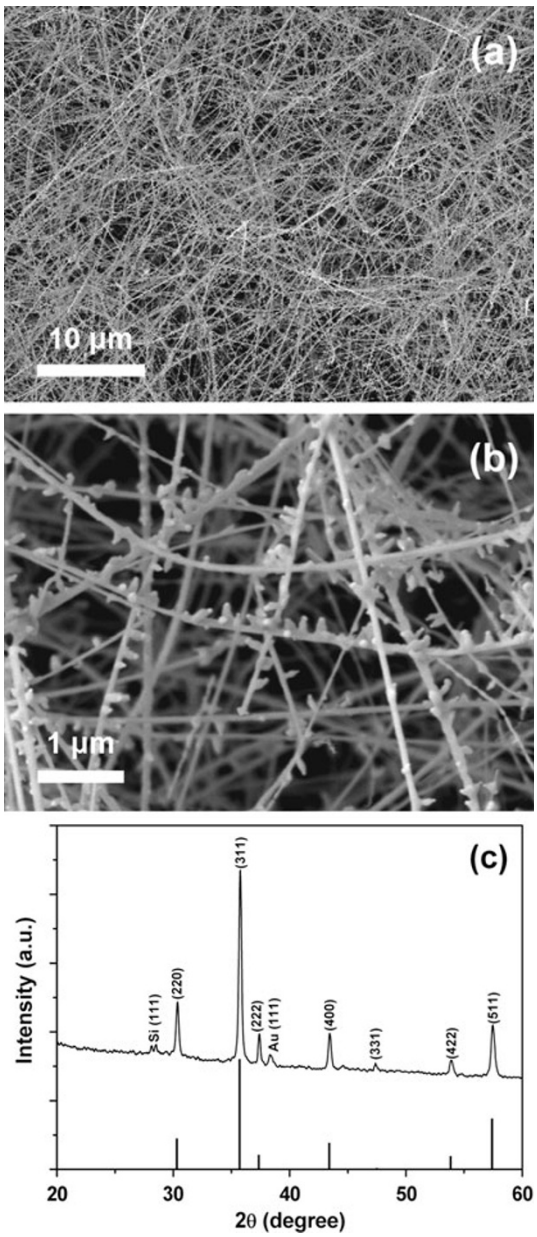

Fig. 2 Characterization of comb-like $ZnGa_2O_4$ nanostructures: **a** low-magnification FE-SEM image; **b** high-magnification FE-SEM image; **c** XRD pattern of as-prepared $ZnGa_2O_4$ nanostructures

(HRTEM) images and the corresponding selected-area electron diffraction (SAED) of region 2 to 4 in Fig. 3a are shown in Fig. 3f–h and the inset to them, respectively, which reveal that the comb-like $ZnGa_2O_4$ nanostructures are highly crystallized. In Fig. 3f, it can be seen that the marked interplanar spacing is 0.48 nm which corresponds to the (111) lattice plane of $ZnGa_2O_4$, indicating the dominant growth direction of the tooth along the [111] direction. And no extended defects were found in the whole tooth. Fig. 3g is the HRTEM image and the corresponding SAED of junction region between the stem and the tooth

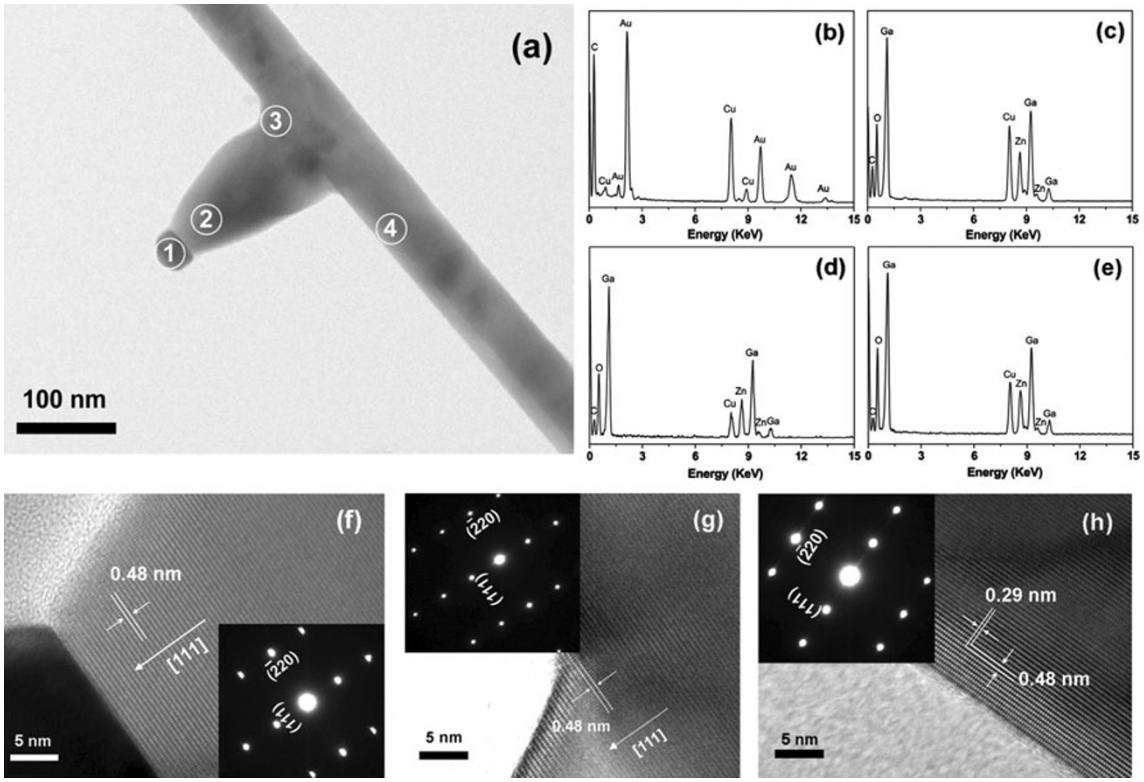

Fig. 3 **a** Typical TEM image of a single-$ZnGa_2O_4$ nanocomb. **b–e** are the EDS spectra acquired from marked regions 1 to 4 in **a**. The HRTEM images and the corresponding SAED of marked regions 2 to 4 in **a** are shown in **f–h** and inset to them, respectively

depicts that the interface is very smooth without planar defects like other semiconductor comb-like nanostructures [31, 32]. It is of advantage to be used in the future application. Figure 3h is the HRTEM image and the corresponding SAED of stem. The marked interplanar spacings are 0.48 and 0.29 nm corresponding to the (111) plane and $(\bar{2}20)$ plane, respectively. It can be inferred that the initial Ga_2O_3 nanowires were totally transformed into highly pure and single-crystalline $ZnGa_2O_4$ nanowires after reacting with Zn and/or ZnO_x vapors at high temperature.

The growth of comb-like $ZnGa_2O_4$ nanostructures follows the VLS process (as shown in Fig. 4). During the previous annealing process, Au nanoparticles have arranged on the side surface of Ga_2O_3 nanowires (Stage I in Fig. 4). During the heating process, the starting material ZnO powder reacted with carbon to form Zn and/or ZnO_x vapors at 850°C. The vapors were carried downstream to the Ga_2O_3 nanowires by Ar gas (stage II in Fig. 4). These vapors deposited on the surface of the Ga_2O_3 nanowires and $ZnGa_2O_4$ stem formed through reaction (stage III in Fig. 4). The orderly arranged Au nanoparticles on the side surface of Ga_2O_3 nanowires seem to be the preferred sites for the growth of $ZnGa_2O_4$ nanoteeth. In the growth process, Zn and/or ZnO_x vapor and the remained O_2 may be absorbed by Au nanoparticles, and Ga in nanowires may also diffuse to these sites. When the alloy droplets got supersaturated, $ZnGa_2O_4$ may nucleate to form the teeth (stage III in Fig. 4). During the heating process, the gradually reaction of Ga_2O_3 nanowires with Zn and/or ZnO_x vapor causes the continuous consumption of Ga source, which results in that the nanoteeth can not growth too long. At the same time, since the mass diffusion of reactant adatoms on the side surface, continuous growth resulting in the formation of tapered teeth (stage IV in Fig. 4). The orderly arranged Au particles on the side surface of Ga_2O_3 nanowires are very important to the growth of $ZnGa_2O_4$ nanocombs. If the annealing process is canceled, no $ZnGa_2O_4$ nanocombs can be obtained as shown in Fig. 5. Under this circumstance, Au first exists as a thin layer on the surface of Ga_2O_3 nanowires. Thus, there are no preferred sites for the growth of teeth. Zn and/or ZnO_x vapors directly reacted with Ga_2O_3 and formed $ZnGa_2O_4$ nanowires. It can be seen that controlling the state and position of Au nanoparticle on the Ga_2O_3 nanowires is the key to obtain $ZnGa_2O_4$ nanostructures with desired comb-like morphology.

The room-temperature PL spectrum of the $ZnGa_2O_4$ nanocomb was presented in Fig. 6. The excitation wavelength is 260 nm. Two emission bands can be observed, which were centered at the 450 and 501 nm, respectively.

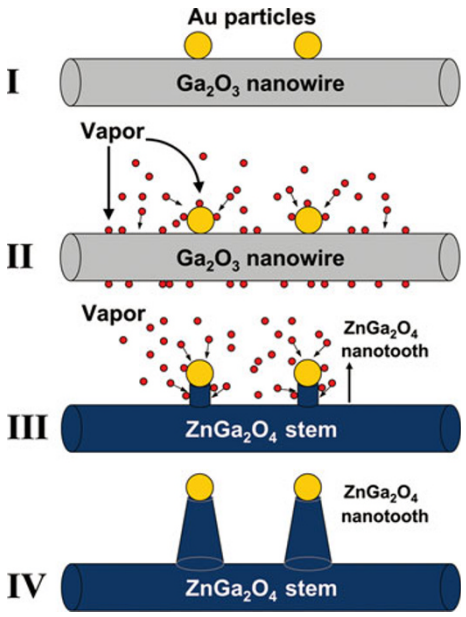

Fig. 4 Schematic illustration of growth process for $ZnGa_2O_4$ nanocombs. *Stage I*: arranged Au nanoparticles on the Ga_2O_3 nanowires after annealing; *Stage II–III*: during the heating process, Au provides preferential site for nucleation and 1-D growth; *Stage IV*: due to the gradually consumption of Ga source and the mass diffusion of reactant adatoms on the side surface, continuous growth resulting in the formation of tapered teeth

The PL spectrum features that the two emission peaks centered at the 450 and 501 nm merged to form a broad band emission ranged from 400 to 575 nm. The PL properties of the $ZnGa_2O_4$ films and nanowires had been investigated intensively [7–9, 22]. From these studies, it can be suggested that the emission band centered at 450 nm may be originated from the self-activation center of the octahedral Ga–O group [7], and the emission band centered at 501 nm may be originated from the electronic transitions of localized Ga^{3+} ion in the octahedral Ga–O group [23]. By comparing with the previous investigation [7–9], it can be suggested the broad band emission in the

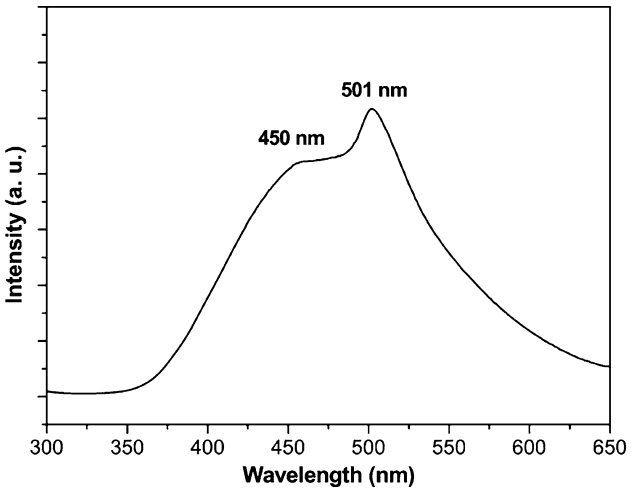

Fig. 6 The room-temperature PL spectrum of comb-like $ZnGa_2O_4$ nanostructure. The excitation wavelength is 260 nm

visible light region of as-prepared $ZnGa_2O_4$ nanocombs may be related to the two-step synthesis method and its hierarchical morphology.

Conclusions

In summary, we present an easy route to synthesize comb-like $ZnGa_2O_4$ nanostructures in a controllable way. The Ga_2O_3 nanowires were used as templates for the following growth of comb-like $ZnGa_2O_4$ nanostructures through the reaction with Zn and/or ZnO_x vapor at high temperature. By annealing Ga_2O_3 nanowires coated with a thin layer of Au film at high temperature, the congregation of Au particles from Au film is the key to the formation of $ZnGa_2O_4$ nanoteeth via VLS mechanism. PL spectra for $ZnGa_2O_4$ nanocombs show a broad band emission in the visible light region from 400 to 575 nm at room temperature. This method can be easily applied to hierarchical nanostructure growth of other materials to enrich the family of low

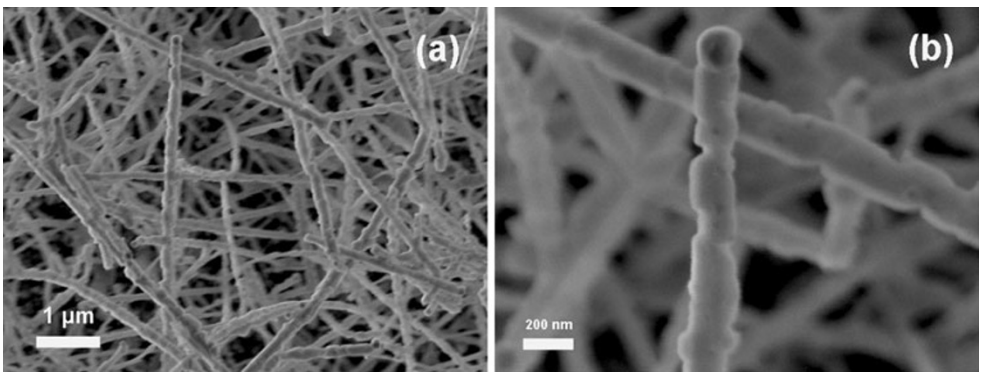

Fig. 5 Low-magnification (**a**) and high-magnification (**b**) SEM images of products obtained without annealing

dimensional nanobuilding blocks and may find potential applications in nanotechnology.

Acknowledgment This work was supported by the National Natural Science Foundation of China (No.50671099, 50172048, 10374090 and 10274085), the Ministry of Science and Technology of China (No.2005CB623603), and the Hundred Talent Program of Chinese Academy of Sciences.

References

1. Y. Cui, C.M. Lieber, Science **291**, 851 (2001)
2. X.F. Duan, Y. Huang, R. Agarwal, C.M. Lieber, Nature **421**, 241 (2003)
3. Z.L. Wang, J.H. Song, Science **312**, 242 (2006)
4. Y.N. Xia, P.D. Yang, Y.G. Sun, Y.Y. Wu, B. Mayers, B. Gates, Y.D. Yin, F. Kim, Y.Q. Yan, Adv. Mater. **15**, 353 (2003)
5. S. Itoh, H. Toki, Y. Sato, K. Morimoto, T. Kishino, J. Electrochem. Soc. **138**, 1509 (1991)
6. T. Omata, N. Ueda, K. Ueda, H. Kawazoe, Appl. Phys. Lett. **64**, 1077 (1994)
7. J.S. Kim, H.I. Kang, W.N. Kim, J.I. Kim, J.C. Choi, H.L. Park, G.C. Kim, T.W. Kim, Y.H. Hwang, S.I. Mho, M.C. Jung, M. Han, Appl. Phys. Lett. **82**, 2029 (2003)
8. I.J. Hsieh, K.T. Chu, C.F. Yu, M.S. Feng, J. Appl. Phys. **76**, 3735 (1994)
9. Y.E. Lee, D.P. Norta, C. Park, C.M. Roulean, J. Appl. Phys. **89**, 1653 (2001)
10. I.K. Jeong, H.L. Park, S.I. Mho, Solid State Commun. **108**, 823 (1998)
11. S.H.M. Poort, D. Cetin, A. Meijerink, G.J. Blasse, Electrochem. Soc. **144**, 2179 (1997)
12. L.E. Shea, R.K. Datta, J.J. Brown, J. Electrochem. Soc. **141**, 2198 (1994)
13. X.N. Zhang, J.H. Huang, K.N. Ding, Y.D. Hou, X.C. Wang, X.Z. Fu, Environ. Sci. Technol. **43**, 5947 (2009)
14. W.W. Zhang, J.Y. Zhang, Z.Y. Chen, T.M. Wang, Catal. Commun. **10**, 1781 (2009)
15. O. Maksimov, Mater. Lett. **62**, 3969 (2008)
16. K.W. Chang, J.J. Wu, J. Phys. Chem. B **109**, 13572 (2005)
17. S.H. Wu, H.C. Cheng, J. Electrochem. Soc. **151**, 159 (2004)
18. S.H. Yang, J. Electrochem. Soc. **150**, 250 (2003)
19. Y.E. Lee, D.P. Norton, J.D. Budai, Appl. Phys. Lett. **74**, 3155 (1999)
20. S.Y. Bae, J.Y. Lee, H.S. Jung, J.H. Park, J.P. Ahn, J. Am. Chem. Soc. **127**, 10802 (2005)
21. Z. Yu, H. Chen, Z.W. Li, Z.M. Yang, H.B. Song, Y.L. Gao, Y.S. Zhang, Y. Jin, Z.F. Jiao, M. Gong, J.G. Zhu, X.S. Sun, Mater. Lett. **63**, 37 (2009)
22. S.Y. Bae, H.W. Seo, W.C. Na, J. Park, Chem. Commun. **16**, 1834 (2004)
23. L. Xu, Y. Su, Q.T. Zhou, S. Li, Y.Q. Chen, Y. Feng, Cryst. Growth Des. **7**, 810 (2007)
24. P. Feng, J.Y. Zhang, Q. Wan, T.H. Wang, J. Appl. Phys. **102**, 074309 (2007)
25. Y.J. Li, M.Y. Lu, C.W. Wang, K.M. Li, L.J. Chen, Appl. Phys. Lett. **88**, 143102 (2006)
26. H.J. Fan, Y. Yang, M. Zacharias, J. Mater. Chem. **19**, 885 (2009)
27. G. Shen, Y. Bando, C.J. Lee, J. Phys. Chem. B **109**, 10779 (2005)
28. G.W. Meng, Y.J. Jung, A.Y. Cao, R. Vajtai, P.M. Ajayan, Proc. Natl. Acad. Sci. **102**, 7074 (2005)
29. M. Misono, Chem. Commun. **13**, 1141 (2001)
30. R.S. Wagner, W.C. Ellis, Appl. Phys. Lett. **4**, 89 (1964)
31. C. Borchers, D. Stichtenoth, S. Muller, D. Schwen, C. Ronning, Nanotech. **17**, 1067 (2006)
32. Y.Q. Wang, U. Philipose, H. Ruda, K.L. Kavanagh, J Mater. Sci. Mater. Electron. **17**, 1065 (2006)